

University of Nebraska - Lincoln

DigitalCommons@University of Nebraska - Lincoln

Norman R. Simon Papers

Research Papers in Physics and Astronomy

1997

The Cepheid instability strip and the calibration of the primary distance scale

Norman R. Simon

University of Nebraska - Lincoln, nsimon@unl.edu

Todd S. Young

University of Nebraska-Lincoln

Follow this and additional works at: <https://digitalcommons.unl.edu/physicssimon>

Simon, Norman R. and Young, Todd S., "The Cepheid instability strip and the calibration of the primary distance scale" (1997). *Norman R. Simon Papers*. 53.

<https://digitalcommons.unl.edu/physicssimon/53>

This Article is brought to you for free and open access by the Research Papers in Physics and Astronomy at DigitalCommons@University of Nebraska - Lincoln. It has been accepted for inclusion in Norman R. Simon Papers by an authorized administrator of DigitalCommons@University of Nebraska - Lincoln.

The Cepheid instability strip and the calibration of the primary distance scale

Norman R. Simon and Todd S. Young

Department of Physics and Astronomy, University of Nebraska, Lincoln, NE 68588-0111, USA

Accepted 1997 February 14. Received 1997 February 12; in original form 1995 September 4

ABSTRACT

This study examines the possibility of galaxy-to-galaxy differences in the long-period Cepheid distributions of external galaxies. A simple theoretical framework is created and linear pulsation calculations are performed to model these distributions. The sturdy nature of the Cepheid period–luminosity (P–L) relation is affirmed, but both analytic arguments and the linear model grids point to potential systematic errors reaching up to a few tenths of a magnitude if the Cepheids in the calibrating and target galaxies have different distributions. We also point out some difficulties posed for stellar pulsation and evolution theory by the long-period Cepheids we have studied: the theoretical blue edge seems too hot and/or the inferred masses too large to account for the observed stars. Preliminary observational evidence is presented which marginally indicates the existence of two somewhat different types of distribution of long-period Cepheids in external galaxies, but further data are needed before this can be confirmed.

Key words: stars: evolution – stars: oscillations – Cepheids – distance scale.

1 INTRODUCTION

Extension of the primary distance scale out to the Virgo cluster and beyond depends upon the long-period Cepheids, which are bright enough to be visible at a great distance. These Cepheids have been calibrated differently by different authors in the literature. Could the distance estimate for a given target galaxy be further deviated from actual if its distribution of long-period Cepheids differs from that of the calibrator? This question was entertained by Simon & Clement (1993), who found, however, that the light curves of the long-period Cepheids in IC 4182 (Saha et al. 1994) could not be distinguished from those in the Galaxy. However, that investigation did not examine the calibration, nor did it treat any other properties of the Cepheids apart from the Fourier parameters characterizing their light curves. At the same time, the error budget of ± 0.20 mag, calculated by the Key Project for both M81 (Freedman et al. 1994a) and M100 (Freedman et al. 1944b), did not include any potential systematic effect originating in differences between the calibrating and target galaxies.

In the present study, we attempt to examine in detail the potential effects on the distance scale caused by differences in the Cepheid distribution from galaxy to galaxy. In Section 2, the possible size of these galaxy-to-galaxy differences is

treated in a simple theoretical framework. In Section 3 we present a large grid of linear pulsation models. Section 4 introduces observational samples and employs the period–magnitude, period–colour and colour–magnitude diagrams in the analysis of the samples. In Section 5, Hertzsprung–Russell (HR) diagrams are plotted and used to point out some problems with the theoretical blue edge. In Section 6, we close with a brief discussion.

2 ANALYTICAL THEORY

We begin with a simple theoretical framework to help us examine possible galaxy-to-galaxy differences in the Cepheid distribution. We want to determine how the distribution of Cepheids in the HR diagram affects distributions in other diagrams (e.g. period–magnitude, period–colour). To infer the relations among the various diagrams let us start with the period/mean-density law from pulsation theory, i.e.

$$\log P = 0.9339 \log L - 0.7678 \log M - 3.540 \log T_e + 11.50, \quad (1)$$

where P is in days, and L and M in solar units. The coefficients in equation (1) represent a fit to a few hundred linear

non-adiabatic (LNA) Cepheid pulsation models constructed for the present study. The model parameters will be described later.

We now supplement equation (1) with a generic mass–luminosity relation for Cepheids evolving through the instability strip. This relation has the form

$$\log L = a \log M + b. \quad (2)$$

Using (2) in (1), we get

$$\log P = a_1 \log L - 3.540 \log T_e + c_1, \quad (3)$$

where

$$a_1 = \left(0.9339 - \frac{0.7678}{a} \right), \quad c_1 = 11.50 + 0.7678 \frac{b}{s}. \quad (4)$$

Suppose now that the distribution of Cepheids in the HR diagram follows the relation

$$\log L = a_2 \log T_e + c_2. \quad (5)$$

Inserting (5) in (3), we obtain

$$\log P = (a_1 a_2 - 3.540) \log T_e + c_1 + a_1 c_2. \quad (6)$$

Now the coefficient a in equation (2) is positive and has a value of about 4.0 (Simon 1995). Thus, the value of a_1 (equation 4) is about 0.74. On the other hand, the typical value one might assign to the coefficient a_2 in equation (5) is -20 or -30 ; this is the slope of the theoretical blue edge (Chiosi 1990). Thus in equation (6), the term $a_1 a_2$ is negative and dominates the slope, which gets steeper as a_2 increases in magnitude. Hence, the steeper the slope in the colour–magnitude diagram (the observational counterpart of equation 5), the steeper will be the slope in the colour–period diagram (the observational counterpart of equation 6).

Finally, we use equation (5) in equation (3) to eliminate $\log T_e$. The result is

$$\log L = \frac{1}{a_3} \log P + c_3, \quad (7)$$

where

$$a_3 = a_1 - \frac{3.4}{a_2}, \quad (8)$$

or

$$M_V = \frac{-2.5}{a_3} \log P + c_4, \quad (9)$$

where M_V is absolute magnitude in the visual bandwidth. If a_2 is large and negative as indicated above, then a_3 is positive, giving the negative slope always observed in the period–magnitude diagram. At the same time one sees from equations (7) and (8) that the larger the magnitude of a_2 , the smaller a_3 and thus the steeper the slope in equation (9). That is, a steep slope in the colour–magnitude diagram gives rise to a steep slope in the period–magnitude diagram. Thus we have demonstrated on general grounds that steep slopes in all the diagrams go together, as do shallower slopes. It remains now to flesh out this picture with an appropriate series of pulsation models.

3 THEORETICAL MODELS

We constructed a large number of linear pulsation models, spanning a wide range of masses, luminosities and temperatures. Five series of models were created, labelled A through E, in accordance with the generic mass–luminosity (M–L) relation given in equation (2). These cases are listed in Table 1, where the progression is generally from lower to higher luminosity at a given mass. The period range we shall study is $10 < P < 60$ d; these are bright Cepheids visible at great distance. The last two columns in Table 1 describe the temperature and mass ranges associated with these periods for each of the cases treated.

Using equations (3) and (4) we may compare the period–luminosity (P–L) relations that would result from the various cases in Table 1. It is easy to discern that for constant period and temperature, the luminosity range spanned by the five cases is about $\Delta \log L = 0.25$, i.e. 0.6 mag, in the sense that case A is brighter than case E. However, the fourth column of Table 1 clearly displays a temperature trend such that, going down the table, each succeeding case produces models which are hotter by about 100 K. Thus the difference between cases E and A at a given period is about 400 K. The effect of this temperature difference is to substantially ameliorate the luminosity spread at constant period, reducing it to about $\Delta \log L = 0.1$, or 0.25 mag. That is, were one to attempt to determine the distance of a group of Cepheids belonging to, say, case E, using as calibration a Cepheid sample belonging to Case A, there would be a systematic error of about 0.25 mag in the distance.

The analytic treatment in the previous sections shows that a steeper (shallower) slope in the HR diagram implies a steeper (shallower) slope in the other diagrams as well, in particular in the period–magnitude diagram. What if we used a galaxy with a ‘steep-sloped’ Cepheid distribution to calibrate a galaxy with a ‘shallow-sloped’ distribution? How much error in the distance might result? This question may be examined using the linear models.

Fig. 1 shows a plot of all the case C models in the magnitude-versus-temperature plane. The straight lines on the diagram select two subsets of the models, one with a sharp, nearly vertical, slope and the other with a milder slope. Let us call these two cuts of the data ‘steep’ and ‘shallow’, respectively.

Table 1. Models according to equation (2).

Case	Range			
	a	b	Te/100K	M/M _⊙
A	3.5	0.40	48 - 54	9 - 15
B	4.0	0.15	50 - 55	7.5 - 12.5
C	4.0	0.40	51 - 57	6.5 - 10
D	4.0	0.65	52 - 58	5.5 - 8.5
E	4.5	0.40	53 - 59	5 - 7.5

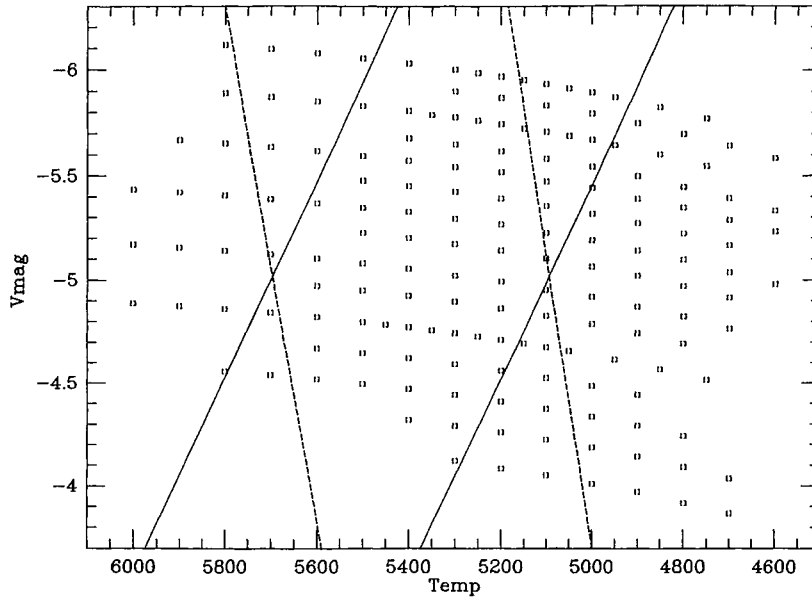


Figure 1. Magnitude versus temperature for the full set of linear pulsation models characterized by case C. Dashed lines contain the ‘steep’ subset; solid lines contain the ‘shallow’ subset.

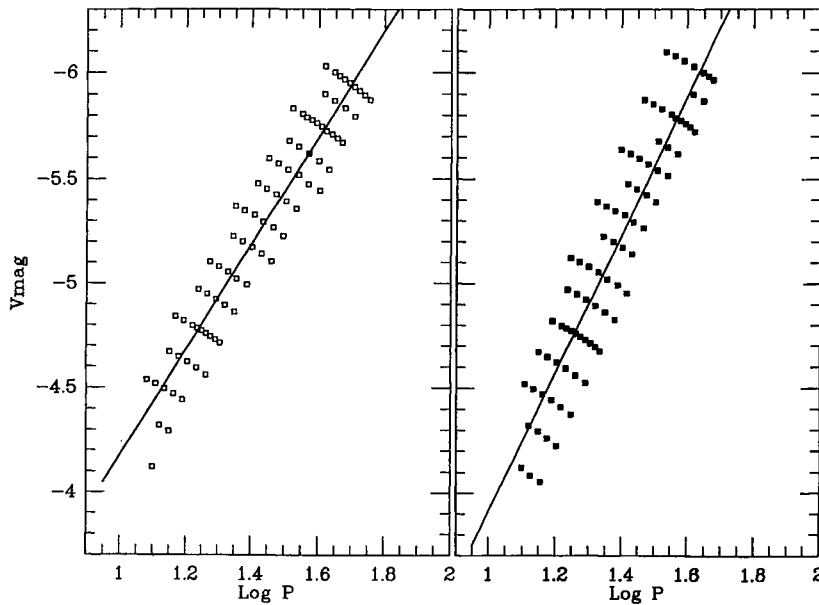


Figure 2. Period–magnitude diagram for the two subsets defined in Fig. 1. Lines are least-squares fits to the points. Right side: ‘steep’ subset; left side: ‘shallow’ subset.

The period–magnitude diagrams for both of the subsets are displayed in Fig. 2. The straight lines are least-squares fits to the shallow cut (open squares, solid line) and the steep cut (filled squares, dashed line), respectively. As expected from the analytic theory in the previous section, the former shows a milder slope and the latter a sharper slope.

The straight lines in Fig. 2 have the form

$$M_V = s \log P + q. \quad (10)$$

Suppose now, as an exercise, that we choose the steep distribution as a calibrator. We force the calibrator’s slope

on the target, make the best fit possible, and note the resulting value of the zero-point q (equation 10), which would determine the distance if the exercise were real. Alternatively, we could choose the shallow distribution as calibrator and go through the same process.

The results of these exercises are given in row 3 of Table 2. Columns 2 and 5 show the ‘correct’ values for the distance determination, since for these cases the target happened to have the same Cepheid distribution as the calibrator. By the same reasoning, the values in columns 3 and 4 are inappropriate because the target and calibrator are different.

Thus along any row of Table 2, comparing columns 2 and

Table 2. Zero-points corresponding to forced-slope fits to theoretical models.

Calibrating Galaxy:	"Steep"		"Shallow"	
Target Galaxy:	"Steep"	"Shallow"	"Steep"	"Shallow"
Case A	-0.59	-0.55	-1.77	-1.74
Case B	-0.46	-0.57	-1.69	-1.77
Case C	-0.61	-0.55	-1.71	-1.69
Case D	-0.58	-0.48	-1.62	-1.53
Case E	-0.46	-0.52	-1.54	-1.62

3 gives some idea of the error one might incur by forcing on a shallow galaxy the calibrating slope corresponding to a steep galaxy. A comparison of columns 4 and 5 illustrates the same potential error when the calibration relation is reversed. On the other hand, reading down any of the columns shows the range of uncertainty occasioned by the possibility that different galaxies have Cepheid distributions characterized by the various cases given in Table 1. One notes that in most circumstances the errors are rather small, the maximum in the table reaching only 0.24 mag (difference between cases B and D, column 5).

We see that both analytic arguments and the detailed fits to LNA pulsation models give 0.25 mag as an estimate of the maximum uncertainty in the distance scale corresponding to the possibility that different galaxies may display different Cepheid distributions. That the range of uncertainty is so small is remarkable considering, particularly, the large differences among the cases in Table 1. Although the Cepheids in a galaxy governed by case A would be twice as massive as those in a case E galaxy, the estimated error incurred by comparing these two galaxies as if they were alike is only a quarter of a magnitude. On the one hand, this argues the essential, impervious nature of the Cepheid P–L relation: no matter how distinct (within reason) the Cepheid distribution in a given galaxy, the standard P–L relation will yield a reliable estimate of distance. On the other hand, our analysis shows that if the Cepheids in a calibrating and a target galaxy have different distributions, the systematic error in the distance could conceivably be as large as the entire error budget assigned by Freedman et al. (1994a,b).

4 OBSERVATIONAL SAMPLES

Let us begin with the 22 long-period Cepheids from the Large Magellanic Cloud (LMC) used by the *Hubble Space Telescope* (HST) Key Project team to calibrate the distance to M81 (Freedman et al. 1994a) and for the initial calibration in the case of M100 (Freedman et al. 1994b). These Cepheids span the period range $10 \leq P \leq 50$ d. In the period–magnitude diagram, a free fit to these stars, with the form of equation (10), yields a slope $s = -3.3$.

Next, we consider a comparable sample of Cepheids from the Small Magellanic Cloud (SMC) in the same period range. This consists of 39 stars with $V-I$ colours listed by Madore (1985). For these stars a period–magnitude fit

Table 3. Fitted slopes (M_V versus $\text{Log } P$) for various LMC and SMC data sets.

LMC	SMC	Difference	Sigma
$-3.3 \pm .28$ (L1)	$-2.5 \pm .20$ (S1)	0.8	0.34
$-3.0 \pm .24$ (L2)	$-2.4 \pm .20$ (S2)	0.6	0.31
$-3.0 \pm .22$ (L3)*	$-2.4 \pm .21$ (S3)*	0.6	0.30
$-3.2 \pm .26$ (L4)*	$-2.4 \pm .20$ (S4)*	0.8	0.33
$-3.1 \pm .24$ (L5)*	$-2.5 \pm .21$ (S5)*	0.6	0.32

*Individual reddenings and tilt included.

Notes

L1: Madore – 22 stars with $V-I$ colours
 S1: Madore – 39 stars with $V-I$ colours
 L2: Madore – 47 stars with $B-V$ colours
 S2: Madore – 65 stars with $B-V$ colours
 L3: Caldwell – 47 stars with $B-V$ colours
 S3: Caldwell – 65 stars with $B-V$ colours
 L4: Caldwell – 17 stars with $V-I$ colours
 S4: Caldwell – 38 stars with $V-I$ colours
 L5: Laney – 30 stars with $B-V$ colours
 S5: Laney – 42 stars with $B-V$ colours

according to equation (10) gives a slope $s = -2.5$. To the Cepheids in the Magellanic Clouds we may add two additional data sets, both from *HST* observations. These are M81 (Freedman et al. 1994a) and IC 4182 (Saha et al. 1994). Interestingly enough, when equation (10) is applied to these two samples, the results are $s = -2.4$ and $s = -3.4$, respectively.

Thus, we see some hint of a dichotomy in the period–magnitude diagrams of the four galaxies treated, namely a sharp slope, $s \simeq -3.3$, for IC 4182 and the LMC, and a shallow slope, $s \simeq -2.5$, for M81 and the SMC. Formal statistical analysis shows that these differences exist at a level of 2σ .

However, this evidence for a dichotomy possesses the inherent limitations of the relatively sparse data sets that we have employed. While the observational sample could not be expanded in the cases of IC 4182 and M81, it was possible to do so for the Magellanic Clouds. Thus we considered a number of enlarged samples as follows: (1) all of the Madore (1985) LMC and SMC Cepheids in the 10 to 50 d range with listed $B-V$ colours; and (2) three data sets kindly provided by David Laney and John Caldwell of the South African Astronomical Observatory. The latter samples had the advantage of including corrections for both the individual reddenings of the program stars and distance effects within the observed galaxies themselves.

Table 3 displays the results of fitting equation (10) to the various samples. Columns 1 and 2 give the fitted slopes, along with standard errors, for comparable data sets in the LMC and SMC, respectively. These data sets are briefly described in the ‘Remarks’ column. In column 3 we list the difference obtained by merely subtracting the LMC from the SMC slope, while column 4 gives the standard error in this difference, calculated by adding quadratically the indi-

vidual errors from columns 1 and 2. We note that in all cases the difference between the two galaxies holds at or above 2σ .

Finally, we studied period–colour and colour–magnitude diagrams for the Cepheids in the various galaxies. In the period–colour plots, there is a hint that the slopes are sharper for the LMC and IC 4182, and milder for the SMC and M81; however, the statistical difference in the slopes lies between 1σ and 2σ . Thus, while this putative difference has the direction predicted by theory, it remains at present an ‘eyeball’ result without solid statistical backing. In the case of the colour–magnitude diagrams, the situation is even more unsatisfactory: the various data sets are sparse and uncertain enough that the Cepheid samples in the four galaxies cannot be distinguished.

5 THE HR DIAGRAM

Our next task will be to convert the extragalactic Cepheid data so it can be plotted on an HR diagram. Given published distances and reddenings for the various galaxies (see Table 4), the absolute visual magnitude of each Cepheid is known. Then, the $\log L$ value for each star becomes a function of the temperature, via the bolometric correction formula given by Simon & Kanbur (1995). (Note that the very small gravity dependence in this formula may be eliminated with virtually no error by taking $\log g = 1.0$.) Thus

$$\log L = f(\log T_e). \quad (11)$$

Now choose one of the cases in Table 1; this fixes a_1 and c_1 (equation 4). Use of these values in equation (3), along with equation (11) and the observed period of the given Cepheid, results in a polynomial equation for $\log T_e$ which may be solved iteratively; then equation (11) gives $\log L$. Thus for any specified choice of an M–L relation, all of our observed sample of extragalactic Cepheids may be rendered on an HR diagram.

Fig. 3 shows such a diagram for case C of Table 1, while Fig. 4 gives it for case A. Cepheids in the different galaxies are represented by different symbols as indicated. In each case the blue edge has also been drawn in as a straight line. We see that if we take the Cepheids to belong to case C, a large number of them are found to lie blueward of the theoretical instability strip, whereas the choice of case A accommodates many more stars. Comparison of Figs 3 and 4 shows that the blue edge changes very little between the

Table 4. Distances and reddenings for four galaxies.

Galaxy	$(m-M)_{true}$	$E(B-V)$	$3.3E(B-V)$	References ¹
LMC	18.50	0.10	0.33	1
SMC	18.90	0.09	0.30	2, 3
M81	27.80	0.03	0.10	4
IC 4182	28.36	0.00	0.00	5

1. Madore & Freedman (1991); 2. Smith et al. (1992); 3. Grieve & Madore (1986); 4. Freedman et al. (1994a); 5. Saha et al. (1994).

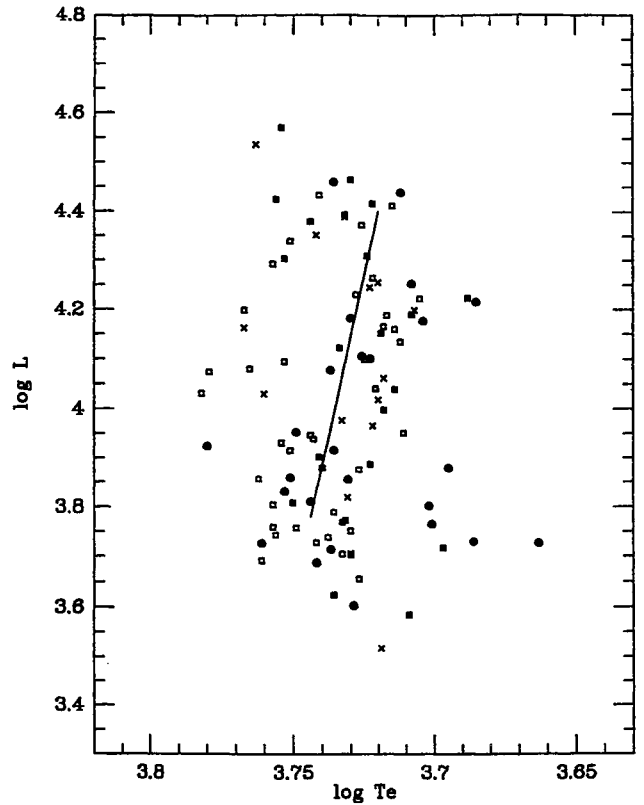


Figure 3. HR diagram for Cepheids in four galaxies, based upon case C. Filled squares: LMC; open squares: SMC; dots: M81; crosses: IC4182. Solid line: blue edge.

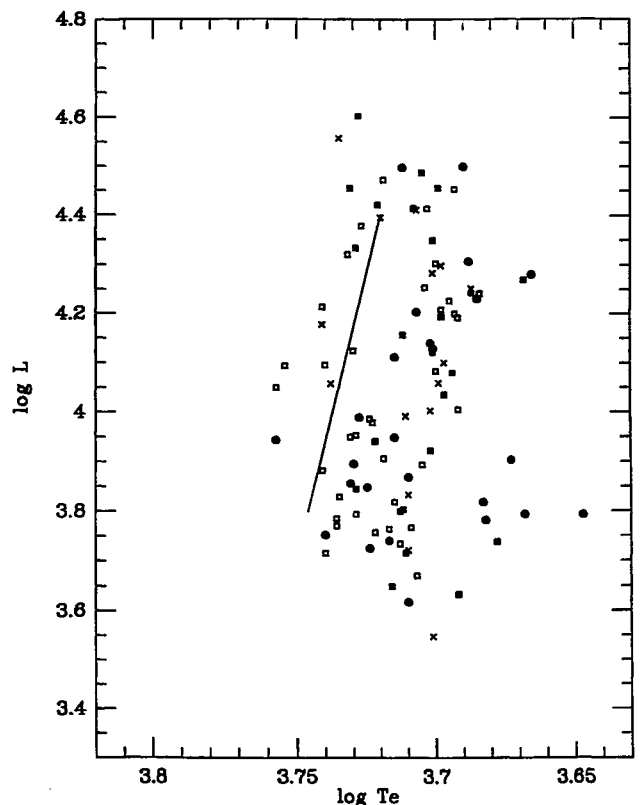


Figure 4. Same as Fig. 3, but based upon case A.

two cases. Rather, it is the cooler inferred temperatures corresponding to case A that are responsible for moving most of the stars into the strip. These cooler temperatures are compensated by significantly higher masses, as can be seen from the last two columns in Table 1. While the stars with low L/M (luminosity per unit mass), corresponding to case A, greatly ameliorate the blue-edge problem, other difficulties are associated with them, as discussed briefly in Section 6, below.

6 DISCUSSION

We have employed analytic theory and linear pulsation models to study the properties of Cepheid distributions in the period–magnitude, period–colour, colour–magnitude and HR diagrams. Circumstantial evidence has been presented for the existence of galaxy-to-galaxy differences in the distribution of long-period Cepheids. Our modelling verifies the extremely sturdy nature of the Cepheid $P-L$ relation, but we also estimate that reasonable differences in the Cepheid distributions of calibrating and target galaxies could result in distance scale errors of a few tenths of a magnitude. However, since the evidence for differing Cepheid distributions among external galaxies remains shaky statistically, more observations will be necessary, particularly on the long-period samples in the Magellanic Clouds.

In addition to the problem of the distance scale, the current investigation also raises questions concerning both pulsation theory and Cepheid evolution. Fig. 3 shows that if the middling evolutionary scenario represented by case C is correct, then the current theoretical value edge must be too cool by 300 to 400 K! This result contradicts some other studies (e.g. Chiosi et al. 1992; Chiosi, Wood & Capitanio 1993), which find adequate agreement between observed and theoretical blue edges. However, these studies proceed differently from ours, particularly in incorporating a colour–temperature conversion at an early stage. We believe such a method to be more precarious, but a debate on this question must be saved for a future work.

If a blue-edge problem really exists, one may ameliorate it by choosing case A, but then other potential difficulties arise. In the first place, we know of no published evolutionary tracks with a luminosity-to-mass ratio as small as that of

case A. Secondly, case A requires that the masses of the long-period Cepheids be very large (9–15 M_{\odot}). This would have to be corrected for in each galaxy with the putative age of the Cepheid sample and the presence or absence of other kinds of stars, including the resonant ‘bump Cepheids’ with periods near 10 d. These and other problems with Cepheid evolution have been discussed by Simon (1995).

Ultimately, we must ask of the theory of stellar evolution that it account for the Cepheid sample in a galaxy of known distance on a star-by-star basis, locating each object along an evolutionary track nested in the instability strip and unfolding on a nuclear time scale. It seems that considerable work will be required before this can be accomplished.

ACKNOWLEDGMENTS

We are pleased to acknowledge support from the NASA Astrophysics Theory Program, under grant no. NAGW-2395, as well as helpful discussions with colleagues at the SAAO, including David Laney, John Caldwell and Luis Balona.

REFERENCES

- Chiosi C., 1990, in Cacciari C., Clementini G., eds, *Confrontation Between Stellar Pulsation and Evolution*. Astron. Soc. Pac., San Francisco, p. 158
- Chiosi C., Wood P., Bertelli G., Bressan A., 1992, *ApJ*, 387, 320
- Chiosi C., Wood P., Capitanio N., 1993, *ApJ*, 86, 541
- Freedman W. L. et al., 1994a, *ApJ*, 427, 628
- Freedman W. L. et al., 1994b, *Nat*, 371, 757
- Grieve G. R., Madore B. F., 1986, *ApJS*, 62, 427
- Madore B. F., 1985, in Madore B. F., ed., *Cepheids: Theory and Observations*. Cambridge Univ. Press, Cambridge, p. 166
- Madore B. F., Freedman W. L., 1991, *PASP*, 103, 933
- Saha A., Labhardt L., Schwengeler H., Macchetto F. D., Panagia N., Sandage A., Tammann G. A., 1994, *ApJ*, 425, 14
- Simon N. R., 1995, in Adelman S. J., Wiese W. L., eds, *Astrophysical Applications of Powerful New Data Bases*. Astron. Soc. Pac., San Francisco, p. 211
- Simon N. R., Clement C. M., 1993, *ApJ*, 419, L21
- Simon N. R., Kanbur S. M., 1995, *ApJ*, 703, 451
- Smith H. A., Silberman N. A., Baird S. R., Graham J. A., 1992, *AJ*, 104, 1430